Actuation system design and control for a scale model unmanned inland cargo vessel

G Peeters[1,2], T Catoor[2], M R Afzal[2], M Kotze[2], P Geenen[2], S Van Baelen[2], M Vanierschot[2], R Boonen[2] and P Slaets[2]

[1] Research Foundation - Flanders (FWO), Egmontstraat 5, 1000 Brussel, Belgium
[2] KU Leuven, Mechanical Engineering Technology Cluster TC, Campus Group T, Andreas Vesaliusstraat 13, 3000 Leuven, Belgium

E-mail: gerben.peeters@kuleuven.be

Abstract. This study describes the design and build of the actuation of an automated scale model inland vessel of type CEMT-I. This suggested design could help to increase the competitiveness of smaller inland vessels which are slowly diminishing. Moreover, this idea aligns with the ambition of the European Commission to increase the cargo flow over waterborne transport. Therefore this study scaled down a newly designed barge of the European project Watertruck$^+$. These barges have a 360-degrees-steerable steering grid in the bow together with a 360-degrees-steerable four-channel thruster at the stern. This configuration unlocks new and more advanced motion control possibilities compared to conventional actuation systems. The performance of this actuation design, at different propeller speeds and angles, was experimentally identified for the scale model. Furthermore, the implemented back-seat driver control paradigm is discussed at its two levels of implementation. Firstly, the lowest level control, to reach certain desired sytem states, is shown. Secondly, the higher level control, the autonomy system provided by the MOOS-IvP software, is discussed and its interaction with the low level control is demonstrated. The authors believe that the combination of this actuation and control design can unlock new cargo transport opportunities for the European inland waterways.

1. Introduction

Over the next decades, the European Commission wants to induce a paradigm shift in the multi-model freight transport sector of the European Union. More precisely, the commission aims at shifting 30% of road freight over 300 kilometres to rail and water-borne transport in 2030 and by more than 50% in 2050 [1]. This envisaged modification would simultaneously tackle the European inland road congestion problem and its accompanying emissions problem by leveraging the fact that the external costs for inland waterway transport (congestion, accidents, noise and emissions) prove to be much lower compared to other modes of transport [2]. Nevertheless, there currently exists an outflow off small inland vessels, type CEMT I-II [3], due to their diminishing economic viability [4], despite the fact that their external costs are generally a factor of five smaller than the external costs for road transport [5]. A large part off the transportation cost of these smaller inland vessels are the crew costs which can rise up to 60% of the total transportation cost [4]. An attempt to decrease the crew costs for smaller vessels has been made by the Watertruck$^+$ project within the Trans-European Transport Network (TEN-T) framework [6]. In its pilot phase, Watertruck$^+$ will introduce 30 new CEMT I-II vessels, both barges and

push boats, to the European inland fleet, which can sail in convoys and can be coupled or decoupled to allow maximal flexibility and modularity. Furthermore, this modular design opens the possibility to separate the time-intensive cargo handling from sailing. A picture of one pushboat sailing with four CEMT I barges is shown in fig 1(a). This study developed a scale model of these push barges shown by fig 1(b), which will serve as a research vessel for increasing the automation of smaller inland vessels.

(a) (b)

Figure 1. Watertruck^{+} convoy of one push boat and four CEMT I barges (a) and the KU Leuven scale model (b).

The first batch of CEMT I vessels have two 360-degrees-steerable thrusters consisting of a steering grid in the bow accompanied by a four-channel thruster at the stern. To illustrate this stern thruster, an image (during its construction phase) is shown in appendix A1. The authors believe that this novel actuation configuration unlocks new motion control possibilities for these inland vessels and paves the way for the future development of unmanned or highly automated vessels which could help to reduce the current sailing costs. This study continuous as follows: section 2 describes the physical actuation design together with its experimental data, which were generated in a towing tank. Afterwards, section 3 examines how the actuation system is controlled and how autonomy systems can interact with the current design. Finally, section 4 concludes this paper and section 5 uncovers the future potential and challenges of this research vessel.

2. Actuation design

Table 1 lists the physical relationships between the CEMT-I prototype and its scale model. The total actuation system was also scaled down geometrically whilst ensuring Froude similarity for its performance.

Table 1. CEMT I dimensions.

	CEMT I	Scale model	
Scale	1	8^{-1}	-
Length	38.50	4.81	m
Breadth	5.05	0.63	m
Draft_{empty}	0.60	0.075	m
Draft_{full}	2.80	0.35	m
Block coefficient	0.95	0.95	-
mass_{empty}	110 000	215	kg
$\text{cargo}_{maxixmum}$	395 000	771	kg
mass_{full}	505 000	985	kg

Figure 2 shows a port-side longitudinal side view of the scale model together with the placement and design of both actuators. As visible, both actuators are completely nested inside the hull. This built-in configuration allows for maximal manoeuvring possibilities for the vessel in the often spatially restricted inland waterways. Both actuators have the same working principle: a propeller sucks in water at the bottom of the hull and then the internal actuation angle θ_i directs the outflow of this water stream. Section 2.1 discusses the full design of the bow thrusters whereas section 2.2 uncovers the stern thruster.

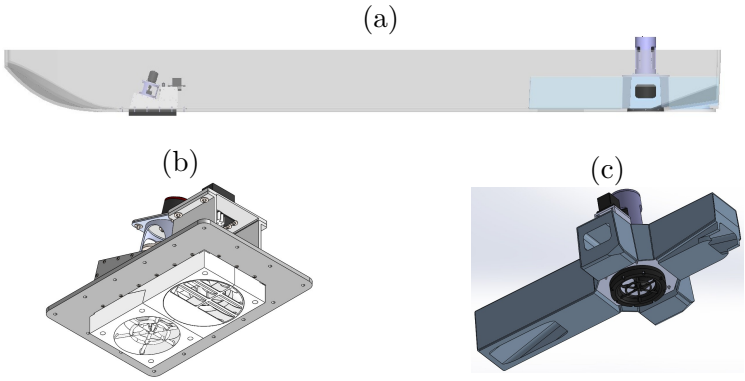

Figure 2. Transparent view of the scale model hull (a), with built-in bow thruster (b) , and stern thruster (c).

2.1. Bow Thruster

The custom-made bow thruster consists of a propeller, which provides the suction power, and a 360-degrees-steerable steering grid, which directs the outflow of water and thus its resulting thrust force T^b. Figure 3 abstractly represents this bow thruster as a top view of the bottom of the vessel hull, for two internal actuation angles $\theta_i^b = 0°$and $90°$. The chosen angle convention directly gives the orientation of the resulting T^b, as the water flow exists the actuator in the opposite direction through the steering grid. The propeller is designed as a Kaplan Series Ka without nozzle and has a diameter of $D^b = 100$mm, a blade area ratio of $B_A^b = 0.65$, and a pitch/diameter ratio of P_D^b =0.95.

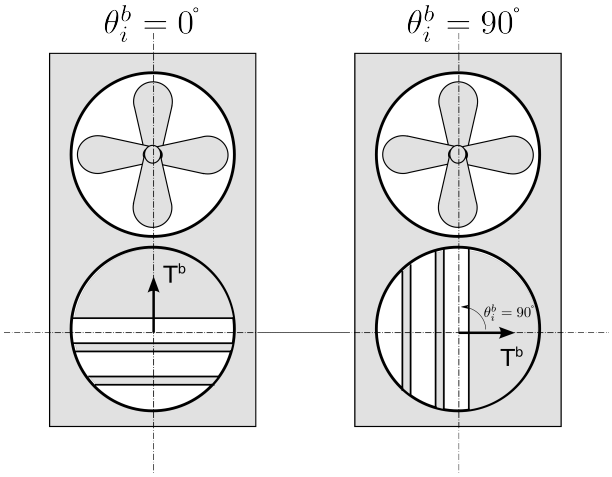

Figure 3. Top view of the bottom section of the hull for $\theta_i^b = 0°$(left) and $90°$(right). Top is oriented to the bow of the vessel, bottom to the stern, consequently the left side points port and the right side starboard.

The resulting thrust forces T^b at different rotational speeds of the propeller shaft n^b and different angles of θ_i^b were measured in a towing tank facility. Figure 4 represents these experimental data. The bow thruster was tested as a separate entity, i.e. not fixed in the ship hull, hence no hull losses were incorporated. Moreover, the tests were conducted at zero speed hence there were

no wake influences. For the bow, the θ_i^b and the output angle θ_o^b of the resulting T^b always aligned, as the water can exit freely under each internal angle. The drop in T^b at θ_i^b $\in$[150°, 180°] could be caused by the fact that at these angles the orientation of the outflow of water is directed towards the propeller where the water gets sucked in. This most likely caused the drop in resulting thrust force as a small closed loop system of water flow might occur. Future work aims at the modelling and further identification of these peculiar zones.

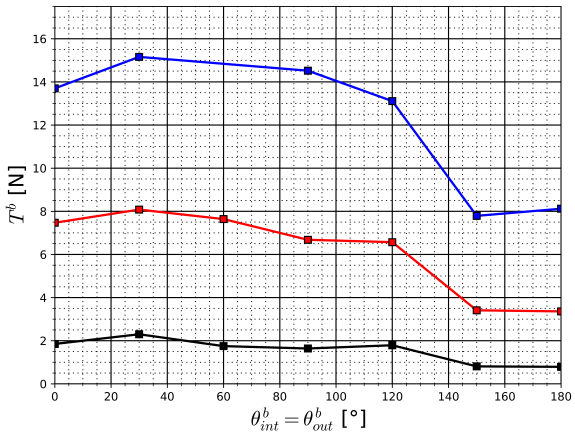

Figure 4. Experimental thrust force results of the bow thruster, T_b. Linearly interpolated at n^b =500 rpm (■——), 1000 rpm (■——), and 1500 rpm (■——).

2.2. Stern thruster

The stern also has a Kaplan Series Ka propeller without nozzle with a blade area ratio of B_A^s = 0.65 and a pitch/diameter ratio of P_D^s =0.95, but with a diameter of D^s = 150mm. Figure 5 shows the working principle of the stern thruster where a similar internal angle convention was chosen for θ_i^s. As demonstrated, the stern has four outlet channels for the water flow and the internal mechanism that directs this flow has an opening of approximately 85°, to assure full closure when the jet is aimed directly into one of the four channels. If $\theta_i^s = 180°$ the water will only flow through the channel pointing at the bow of the vessel, resulting in a backwards thrust force T^s. However, when $\theta_i^s = 45°$ the water outflow can enter two channels, one pointing stern and the other one pointing port.

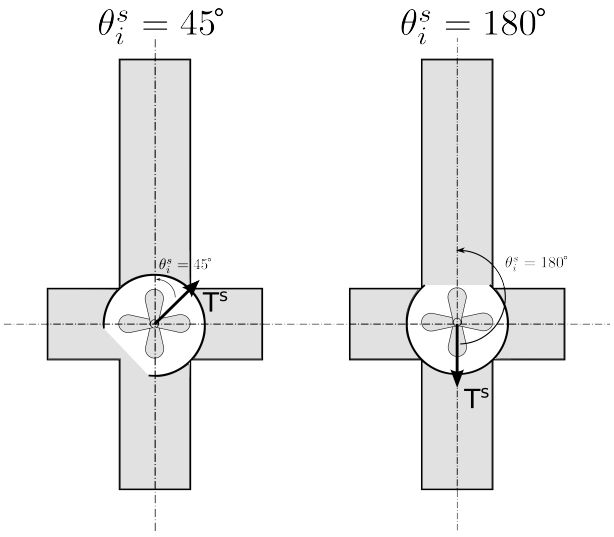

Figure 5. Top view stern thruster, top aims at bow, bottom at stern, left at port and right at starboard. Internal actuation angle $\theta_i^s = 45°$ (left) and $= 180°$ (right).

Due to the asymmetric design of the length and shape of the outflow channels, the outlet angle θ_o^s of the resulting thrust force will not always align with the θ_i^s angle. This discrepancy between θ_i^s and θ_o^s introduces a non-linear mapping between both angles, illustrated by fig 6. This non-linear mapping seems to be reproducible as it occurs similarly at five different shaft speeds n^s of the stern propeller. The experimental data for the stern thruster were taken at different shaft speeds close to, but never exactly, 300, 600, 900, 1200, and 1500 rpm and kept constant over the complete θ_i^s domain. The stern propulsion system was placed inside the ship hull during its identification, hence the hull coefficient is indirectly included into the measurements. These tests were also conducted at zero speed, hence no wake influences were measured.

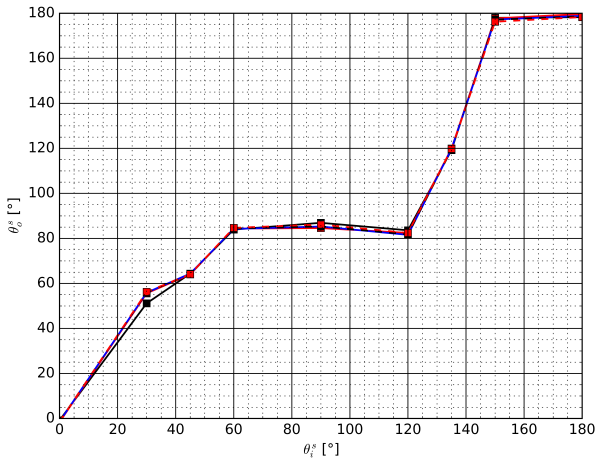

Figure 6. Non-linear mapping between θ_i^s and θ_o^s, linearly interpolated at n^s ±300 rpm (■——), ±600 rpm (■——), ±900 rpm (■——), ±1200 rpm (■- - -), and ±1500 rpm (■- - -).

The stern thrust force, T^s, was orthogonally decomposed into T_x^s and T_y^s on the longitudinal and transversal axes of the vessel respectively, with the origin placed at the center of the rotational axis of the stern propeller shaft, resulting in the following relationships:

$$T^s(n^s, \theta_i^s) = \sqrt{T_x^s(n^s, \theta_i^s)^2 + T_y^s(n^s, \theta_i^s)^2}, \quad \theta_o^s = \arctan\left(\frac{T_y^s}{T_x^s}\right) \tag{1}$$

Figure 7 summarises the experimental data for the stern actuation. T_x^s has a dead zone for $\theta_i^s \in [60°, 120°]$, which most likely causes the non-linearity in the mapping of fig 6 within the same θ_i^s range. Likewise, a similar behaviour and relationship with fig 6 can be noted for the lateral thrust force T_y^s for $\theta_i^s \in [150°, 180°]$. Future work aims at modelling the orthogonally decomposed T^s whilst incorporating its dead zones.

3. Vessel Control

The vessel can be remotely steered by accessing its Programmable Logic Computer (PLC) through a web interface. On this interface, the desired propeller speeds and internal actuation angles can be set. The PLC then drives the actual speeds and angles to these desired states, this process is called low level control (section 3.1). These desired system states can also be provided by an autonomy system, named the high level control (section 3.2). Furthermore, in the future, a physical remote control will be connected to the PLC to manually steer the vessel.

3.1. Low level control

Figure 8 shows the communication links between the PLC and the total actuation system in order to perform the low level control. The PLC steers the desired propeller shaft speeds $n_{desired}^s$ and $n_{desired}^b$ over a CAN bus network to their respective motor drives, which then translate this

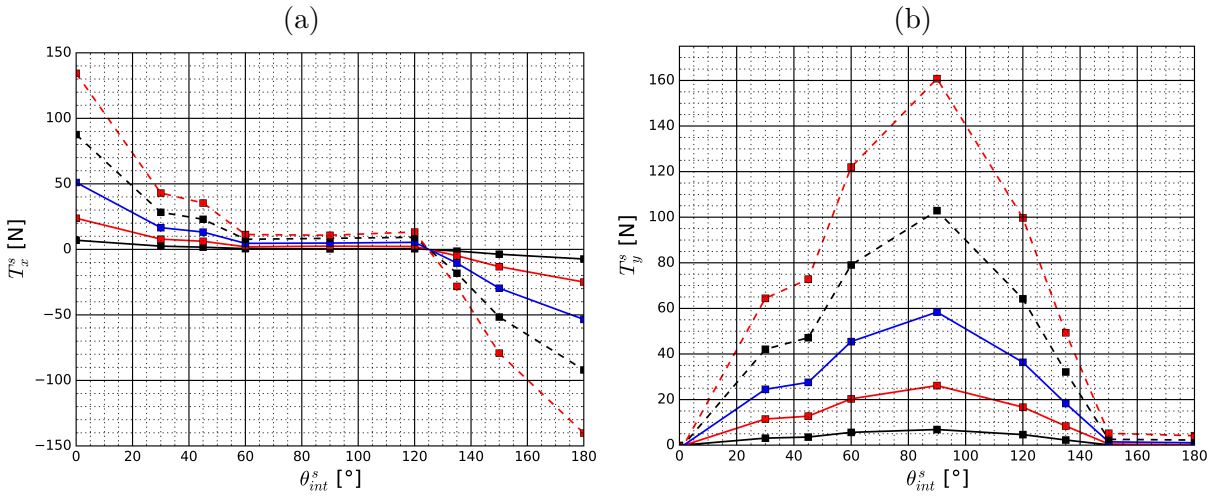

Figure 7. Longitudinal and transversal experimental thrust components T_x^s (a) and T_y^s (b), linearly interpolated at ±300 rpm (■——), ±600 rpm (■——), ±900 rpm (■——), ±1200 rpm (■- - -), and ±1500 rpm (■- - -).

request to the required power for the motors of the propellers. These two motor drives have an internal control loop to push their current speeds to their desired values. The other entity on the CAN bus network, the bow stepper, controls the angle of the steering grid, θ_i^b, by reading its own embedded encoder. The control angle of the stern thruster, θ_i^s, gets read by an external absolute encoder and gets set by controlling the stern stepper drive, which moderates the power for the stern stepper. Additionally, the PLC has a Modbus TCP/IP communication line with an industrial computer on which an autonomy system is nested. This configuration allows for a high level of modularity on the one hand, and levers the industrial robustness of the PLC on the other hand, as it is always possible to overrule the autonomy system and steer remotely.

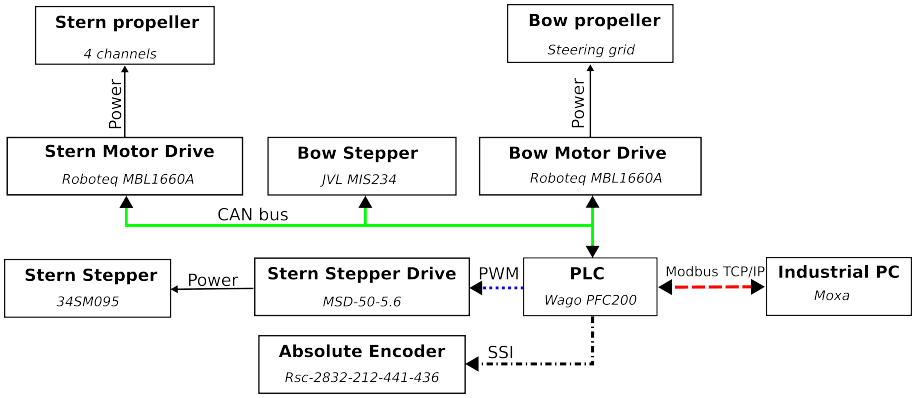

Figure 8. Communication links between the PLC and the actuation system.

3.2. High level control

The above-mentioned modularity in the control design enables the implementation of the back-seat driver paradigm offered by the Mission Oriented Operations Suite - Interval Programming (MOOS-IvP) software. This software offers a set of open source C++ modules to facilitate the automation of robotic platforms with a special focus on autonomous marine vehicles [7]. This MOOS-IvP has the MOOS core as a backbone, which entails a cross platform software

for robotics research in general [8]. The left side of fig 9 shows the idea behind the back-seat driver paradigm: an autonomy system receives navigational information from a vehicle, which it considers as a black box, and then makes autonomous decisions, based on its internal configuration, of which it sends the results back to the vehicle as desired states. The right hand side of this figure depicts the implementation of this paradigm tailored down for the scale model vessel (of which all lower level processes are under also control). In this study, a MOOS application (MOOSApp) called the IvP-Helm (which is provided by the MOOS-IvP) acts as the decision maker of the autonomy system that receives the current states of the vessel and decides about its future by generating the desired states. The configuration of the IvP-helm falls out of the scope of this study. Next, a control MOOSApp will use the current and desired states to generate the lowest level control variables $n^{b,s}_{desired}$ and $\theta^{b,s}_{i,desired}$. Both these processes, the control MOOSApp and the IvP-Helm run on the industrial computer and are asynchronously connected via a MOOS database (MOOSDB). Another client on the MOOSDB will send the desired states over the Modbus TCP/IP connection to the low level PLC, which then uses this information to complete its control cycle.

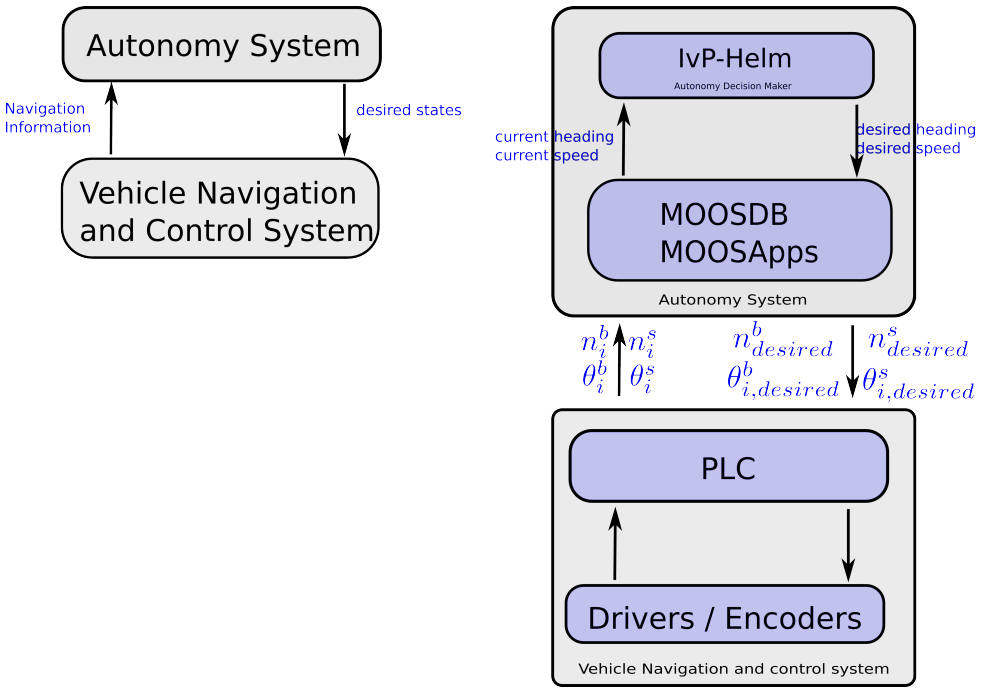

Figure 9. Backseat driver paradigm (left), and its implementation in this study (right).

4. Conclusion

In summary, this paper argued that increasing the level of automation of smaller inland vessels could increase their competitiveness in the inland cargo transport sector. The authors believe that this rise in automation could align with the European project Watertruck$^+$. Consequently, a scale model of a CEMT-I vessel from this project was built. This vessel has a novel actuation configuration, which envelopes two 360-degrees-steerable thrusters, that unlocks a spectrum of new control methodologies for inland cargo vessels. This study showed the first experimental thrust force characteristics of this innovative actuation design. Afterwards, the integration of the actuators in the back seat driver control paradigm was discussed at its two inherent levels

of control. The combination of this control paradigm together with this novel actuation design offers the possibility for the realisation of future unmanned vessels in the European inland waterways.

5. Future work

Although this study has laid the physical foundation for a future unmanned inland cargo vessel, further research steps are needed to fully accomplish this idea. Firstly, positional information needs to be added to the vessel by, for example, a Global Navigation Satellite System (GNSS) sensor of which the performance can be increased by fusing it with an Inertial Measurement Unit (IMU). Together with the above-mentioned control philosophy, this could allow the vessel to sail unmanned in conditioned areas with only static objects. To add dynamic objects in the surroundings of the vessel, sensors providing situational awareness are needed, for example a stereo camera system and, or, a Laser Imaging Detection And Ranging (LiDAR) sensor. A final step would be to share sufficient information with the surrounding vessels and infrastructure in order to safely navigate the inland waterways.

Acknowledgments

The Flanders research foundation funds the doctoral scholarship of Gerben Peeters, project: <1S12517N>. The scale model vessel has been built during the EFRO-Flanders GTI project: <Autonoom varen in de Westhoek>.

Appendix A.

Figure A1. Construction phase 360-degrees-steerable four-channel stern thruster on a CEMT-I.

References

[1] European Commission 2011 Transport 2050: Commission outlines ambitious plan to increase mobility and reduce emissions 2011
[2] Al Enezy O, van Hassel E, Sys C and Vanelslander T 2017 *Research in Transportation Business & Management* **23** 64-74
[3] European Conference of Ministers of Transport 1192 Resolution No. 92/2 on New Classification of Inland Waterways European Council of Ministers of Transport
[4] Sys C and Vanelslander T 2011 *Future Challenges for Inland Navigation* ISBN 978 90 5487 845 4
[5] van Essen H, Schroten A, Otten M, Sutter D, Schreyer C, Zandonella R, Maibach M, and Doll 2011 *External costs of transport in Europe* Delft International Union of Railways UIC.
[6] European Commission Directorate General for Mobility and Transport 2016 *MENA Report* Albawaba Londen
[7] Benjamin M, Schmidt H, Newman P and Leonard J J 2010 *Journal of Field Robotics* **27(6)** 834-75
[8] Newman P 2008 MOOS - mission oriented operating suite *Massachusetts Institute of Technology* 2299